6th International Conference on Advances in Experimental Structural Engineering
11th International Workshop on Advanced Smart Materials and Smart Structures Technology
August 1-2, 2015, University of Illinois, Urbana-Champaign, United States

Fatigue Crack Monitoring using Large-area, Flexible Capacitive Strain Sensors

X. Kong[1], J. Li[2], S. Laflamme[3], and C. Bennett[4]

1 *Graduate Research Assistant, Dept. of Civil, Environmental and Architectural Engineering, University of Kansas, United States.*
E-mail:xkong@ku.edu
2 *Assistant Professor, Dept. of Civil, Environmental and Architectural Engineering, University of Kansas, United States.*
E-mail:jianli@ku.edu
3 *Assistant Professor, Dept. of Civil, Construction, and Environmental Engineering, Iowa State University, United States.*
E-mail:laflamme@iastate.edu
4 *Associate Professor, Dept. of Civil, Environmental and Architectural Engineering, University of Kansas, United States.*
E-mail: crb@ku.edu

ABSTRACT
Strain-based measurements can serve as an effective method for monitoring fatigue cracks. However, traditional metal foil gauges are often not able to capture fatigue crack growth due to their limited measurement range, small size, and high failure rate under harsh environments. Recently, a newly-developed soft elastomeric capacitor (SEC) has shown great promise to overcome these limitations. Inspired by biological skin, this new sensor can transduce strain into changes in capacitance. In this paper, a revised electromechanical model of the SEC sensor is established as an accurate sensing principle for bi-directional strain fields. A comparative study based on finite element analysis verified the performance of the revised electromechanical model. Moreover, the capability of the SEC sensor to detect fatigue cracks in small-scale steel specimens was experimentally investigated. An SEC was attached to a compact tension steel plate subjected to fatigue loading. The capacitance of the sensor and the crack size were measured throughout the test. Results showed that the SEC is capable of detecting crack growth by monitoring a steady increase of its capacitance response.

KEYWORDS: *Structural health monitoring, fatigue crack detection, sensing principle, capacitive sensor*

1. INTRODUCTION

Structural safety of existing bridges is of critical concern to governments, drivers, and pedestrians. In particular, fatigue cracks that occur on metallic structures due to repetitive loading greatly affect bridges' lifespans [1]. Fatigue cracks can be difficult to detect when they are small in size. However, depending upon loading conditions and structural types, these fatigue cracks may grow rapidly and lead to catastrophic structural failure.

Crack monitoring of steel structures has been attempted using various techniques. Park et al. [2] used piezoelectric sensors to monitor crack growth in a structural component of a steel bridge. Utilizing a similar concept, Roberts [3] applied ultrasonic sensors on a T-section girder to detect crack activities. The main concern regarding these approaches, however, is that additional actuators are required to generate a source signal, which increases the complexity of the monitoring system, making them less attractive for long-term autonomous monitoring. After all, fatigue cracks may develop between scheduled inspection dates and can go undetected before a catastrophic failure occurs. Strain-based approaches are another promising solution for crack detection. Two feasibility studies led by Kamaya [4, 5] showed that the growth of a crack inside a metallic container could be successfully captured by observing the container's outside strain variation using strain gauges. Nevertheless, strain gauges have very limited capability for capturing crack activities due to their limited size and measurement range. Recently, new types of large strain-sensing sheets have been developed to monitor fatigue cracks over a large surface. Yao [6] et al. developed a large strain-sensing sheet based on Large Area Electronics to detect and localize crack activities. The results indicated that this particular strain-sensing sheet could capture crack growth and localized damage by measuring strain using the sensing sheet. Nonetheless, significant improvements in terms of reliability and robustness are required before the sensing sheet can be applied in real-world structures.

Recently, a large-size, flexible capacitive strain sensor has also shown great promise in monitoring crack growth through direct strain measurement. Also known as soft elastomeric capacitor (SEC) sensor, this soft and stretchable sensor is capable of measuring a much wider range of strain (up to 20%) compared with traditional foil gauges. Moreover, a larger attachment area of the sensor makes it better suited for crack monitoring over large

surface areas. Laflamme et al. [7, 8] applied this SEC sensor in a RC beam and an aluminum beam, both loaded in flexure. Test results showed that the SEC sensor could accurately monitor structural deformations by converting the measured capacitance response into strain variation. A further study [9] on a CT specimen under fatigue loading demonstrated the capability of the SEC sensor for fatigue crack monitoring. Additionally, a finite element (FE) analysis [10] on the same CT specimen was used to establish a relationship between capacitance response and crack width. However, since only one crack size was measured during each test, the numerical relationship could not be fully verified. The goal of this paper is to experimentally depict the relationship between crack size and capacitance measurement for the CT specimen through an improved test procedure. The next step will be validation of the numerically-derived relationship based on experimental results.

This paper is arranged as follows: Section 2 introduces the background of the SEC sensor development, followed by a revised electromechanical model developed for the SEC sensor subjected to bi-directional deformations. A procedure for applying the revised sensing principle in FE analysis for highly non-uniform strain fields is then described, followed by a comparative study used to verify the accuracy of the revised model; Section 3 presents an experimental study based on a fatigue test of a CT specimen with an attached SEC sensor. The test procedure is improved based on the previous experimental work, aiming to develop a quantitative relationship between crack growth and sensor response. Conclusions are drawn in Section 4.

2. THE SEC SENSOR AND SENSING PRINCIPLES

In this section, the background of the SEC sensor development is introduced. Then, some existing sensing principles are discussed. Based on one existing electromechanical model, a revised model is proposed in order to provide a precise relationship between the capacitance response of the SEC sensor and measured strain.

2.1. The SEC Sensor

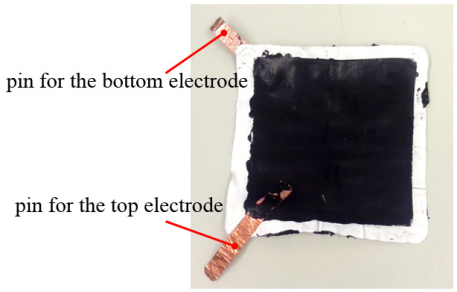

Figure 2.1 The SEC sensor

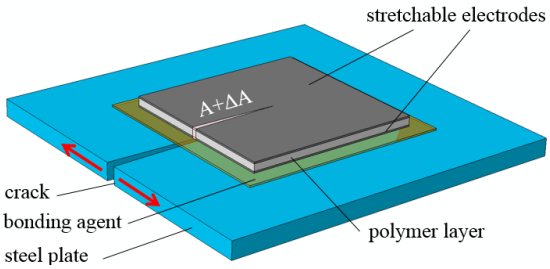

Figure 2.2 Schematic of the SEC sensor applied over a cracked steel plate

The SEC sensor is a large-size capacitor with three polymer layers in a sandwiched structure (Fig. 2.1). The top and bottom layers are stretchable electrodes containing a conductive material, while the middle dielectric layer is made of a nonconductive polymer mixed with titania. A schematic of the SEC sensor is shown in Fig. 2.2. The SEC sensor converts strain change into capacitance change according to the following equation:

$$C = \frac{e_0 e_r A}{h} \tag{2.1}$$

where C is the capacitance of the SEC sensor, e_0 and e_r are the permittivity of vacuum and the polymer, respectively, A and h are the area and thickness of the effective dielectric, respectively. As illustrated in Fig. 2.2, crack activity in the steel plate causes an increased attachment area A and a decreased thickness h, leading to a larger capacitance. More details of the SEC sensor including its fabrication process can be found in [7] and [8].

2.2. Existing Sensing Principles

A sensing principle is fundamental to understanding how the SEC sensor works. Even though the basic principle of the SEC sensor is described in Eq. 2.1, an electromechanical model is needed for strain sensing. On the other hand, such a model also facilitates numerical simulation of the capacitance response of the SEC sensor. Laflamme et al. [8] provided the following equation for the case of uniaxial strain:

$$\frac{\Delta C}{C} = 2\varepsilon_m \tag{2.2}$$

where C and ΔC are the initial capacitance and total capacitance change of the SEC sensor, respectively, and ε_m is the monitored strain. In the following discussion, $\Delta C/C$ is referred to as capacitance response of the SEC sensor. In the case of bidirectional strain, a similar model was also given [11]:

$$\frac{\Delta C}{C} = \frac{1}{1-\nu}\left(\varepsilon_x + \varepsilon_y\right) \tag{2.3}$$

where ε_x and ε_y are strains in the two principal axes, and ν is the Poisson ratio of the dielectric material with a typical value of 0.49. This model can directly convert strain variation into capacitance response. Nevertheless, Eq. 2.3 applies to the case of uniform strain and is difficult to be verified in experiments where non-uniform strain is typical. Moreover, in the derivation, higher-order strain terms such as $\varepsilon_x \times \varepsilon_y$ are neglected, which can underestimate capacitance response when the SEC sensor is subjected to high strains that are typical when cracking occurs.

2.3. A Revised Electromechanical Model

In this section, a revised electromechanical model is established to provide an accurate relationship between capacitance response, $\Delta C/C$, and strain. As shown in Fig. 2.3, consider a micro unit of the SEC sensor. The unit is small enough such that strain under the unit can be considered uniform. X, Y, Z are the three principal strain axes of the micro unit. As shown in the figure, an increased attachment area of the micro unit due to deformation leads to larger length L and width W and a smaller thickness h. Thus, the capacitance response, $\Delta C/C$, can be expressed as:

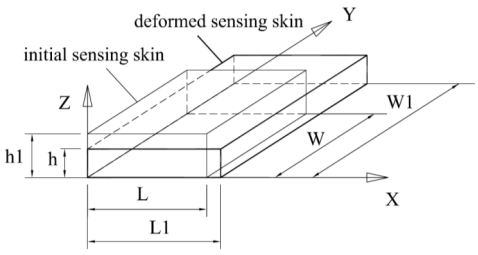

Figure 2.3. A micro unit of a SEC sensor

$$\frac{\Delta C}{C} = \frac{C_1 - C}{C} = \frac{e_0 e_r \left(\frac{A_1}{h_1} - \frac{A}{h}\right)}{e_0 e_r \frac{A}{h}} = \frac{A_1 h - A h_1}{A h_1} \tag{2.4}$$

where C and C_1 are the initial and final capacitance values of the micro unit, A and h are the initial sensing area and the thickness of the micro unit, and A_1 and h_1 are the corresponding results after deformation. Substituting $A=LW$ and $A_1=L_1W_1$ into Eq. 2.4, the capacitance response $\Delta C/C$ becomes

$$\frac{\Delta C}{C} = \frac{L_1 W_1 h - LWh_1}{LWh_1} \tag{2.5}$$

Notice that changes in the geometric dimensions in the micro unit of the sensing skin also indicate strain variations in principal axes, which can be expressed as $L_1=(1+\varepsilon_x)L$, $W_1=(1+\varepsilon_y)W$, and $h_1=(1+\varepsilon_z)h$. Substituting these three equations into Eq. 2.5, the capacitance response $\Delta C/C$ becomes

$$\frac{\Delta C}{C} = \frac{(1+\varepsilon_x)(1+\varepsilon_y)}{(1+\varepsilon_z)} - 1 \tag{2.6}$$

Assuming the sensing skin material is incompressible [8], i.e., $LWh = L_1 W_1 h_1$, and noticing that $L_1=(1+\varepsilon_x)L$, $W_1=(1+\varepsilon_y)W$, and $h_1=(1+\varepsilon_z)h$, the following expression is determined:

$$\frac{1}{1+\varepsilon_z} = (1+\varepsilon_x)(1+\varepsilon_y) \tag{2.7}$$

Substituting Eq. 2.7 into Eq. 2.6, the capacitance response, $\Delta C/C$, of the micro unit of the sensing skin is updated as:

$$\frac{\Delta C}{C} = (1+\varepsilon_x)^2 (1+\varepsilon_y)^2 - 1 \tag{2.8}$$

Eq. 2.8 is the final form of the revised electromechanical model. This model describes the relationship between capacitance response and strain variation in two principal axes. When the strain level is small, higher order terms in Eq. 2.8 can be ignored, leading to the previous sensing principle in Eq. 2.3. However, for large strains, keeping the higher order terms of Eq. 2.8 provides a more accurate solution of capacitance response than Eq. 2.3.

2.4. Application of the Revised Model in FE Analysis

In Section 2.3, a revised electromechanical model was established for the micro unit of the SEC sensor. For bi-directional strain cases such as a steel plate with fatigue cracks, the strain field under the sensing skin is highly localized and non-uniform. In this section, we demonstrate how to use the revised model to simulate the capacitance response of an SEC sensor under non-uniform bi-directional strain through FE analysis.

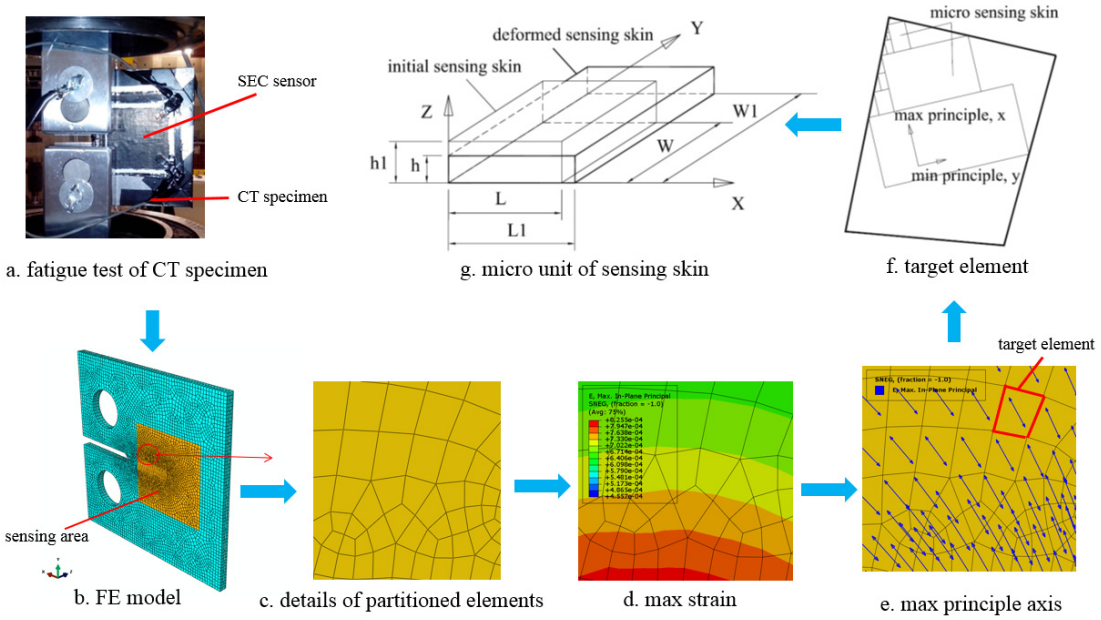

Figure 2.4 Application of the revised model in FE analysis

Fig. 2.4 shows a step-by-step schematic for applying the revised model in an FE analysis. Each element in the FE model is considered small enough such that the strain field is uniform within that element, hence Eq. 2.8 can be applied. To simulate a crack detection experiment (Fig. 2.4a) that included an SEC sensor attached to a steel compact tension (CT) specimen, an FE model of the CT specimen (Fig. 2.4b) was built in Abaqus (version 6.13) [10]. According to Eq. 2.8, the capacitance response of the SEC sensor is a function of ε_x and ε_y from the measured surface. Hence, instead of physically modeling a very thin SEC layer, the sensing area where the SEC sensor was attached was created in the model through partitioning the CT specimen, as shown by the yellow area in Fig. 2.4b. After the FE analysis was completed, each element in the model exhibited its maximum and minimum principal strains. Figs. 2.4d and 2.4e show typical results for max principal strain and its directions in each element.

For a target element with an arbitrary shape shown in Fig. 2.4e, Eq. 2.8 can still be applied even though the principal strain directions are not aligned with the sides of the geometric shape of the element. As a proof, partition this target element into small rectangular micro units with the two sides aligned with the principal strain axes (Fig. 2.4f). Letting the total number of micro units be j, the capacitance for each micro unit can be written as:

$$\frac{\Delta C_j^t}{C_j^t} = (1+\varepsilon_{x,j}^t)^2(1+\varepsilon_{y,j}^t)^2 - 1 \tag{2.9}$$

where ΔC_j^t and C_j^t represent the capacitance change and the initial capacitance of the j^{th} micro unit of the target element. The total capacitance response of the target element (Fig. 2.4f) can be written as a summation of all the micro unit elements:

$$\frac{\Delta C^t}{C^t} = \frac{1}{C^t}\sum_{j=1}^{J}\Delta C_j^t = \frac{1}{C^t}\sum_{j=1}^{J} C_j^t\left[(1+\varepsilon_{x,j}^t)^2(1+\varepsilon_{y,j}^t)^2 - 1\right] \tag{2.10}$$

Assuming ε_x and ε_y are constant in the target element, Eq. 2.10 can be rewritten as

$$\frac{\Delta C^t}{C^t} = \left[(1+\varepsilon_x^t)^2(1+\varepsilon_y^t)^2 - 1\right]\left(\sum_{j=1}^{J} C_j^t \Big/ C^t\right) \tag{2.11}$$

since $\sum_{j=1}^{J} C_j^t \Big/ C^t = 1$, we have the total capacitance of an arbitrary target element as

$$\frac{\Delta C^t}{C^t} = (1+\varepsilon_x^t)^2(1+\varepsilon_y^t)^2 - 1 \tag{2.12}$$

Eq. 2.12 indicates that the revised electromechanical model can be applied to a target element with an arbitrary shape, as long as strain is uniform in this element. Similarly, the total capacitance response of the whole sensing area in Fig. 2.4b can be obtained by the summation of each individual element's result. By assuming there are *I* elements in the sensing area, the total capacitance response of the SEC sensor can be written as

$$\frac{\Delta C}{C} = \frac{1}{C}\sum_{i=1}^{I}\Delta C_i = \sum_{i=1}^{I}\frac{C_i}{C}\left[(1+\varepsilon_{x,i})^2(1+\varepsilon_{y,i})^2 - 1\right] \tag{2.13}$$

Since $C_i/C = A_i/A$, we have

$$\frac{\Delta C}{C} = \sum_{i=1}^{I}\frac{A_i}{A}\left[(1+\varepsilon_{x,i})^2(1+\varepsilon_{y,i})^2 - 1\right] \tag{2.14}$$

Eq. 2.14 enables numerical simulation of the total capacitance response of an SEC sensor subject to a highly non-uniform and bi-directional strain field based on FE analysis. Once the results of principal strains and initial area of each element are calculated, the total capacitance response can be computed.

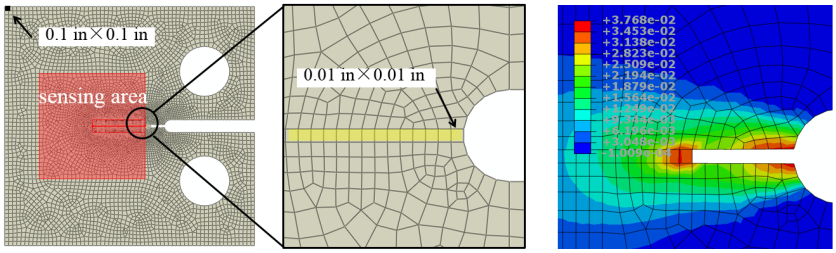

(a) (b) (c)

Figure 2.5 (a) The overall FE model; (b) an inset showing the path of the potential crack; and (c) typical strain result around the crack tip

2.5. Verification of the Proposed Sensing Principle

A comparative study was carried out to verify the accuracy of the proposed sensing principle (Eq. 2.8) as well as the original one (Eq. 2.3). The procedure shown in Fig. 2.4 was adopted for this purpose. An Abaqus model of a CT specimen (Fig. 2.5a) enabled the computation of capacitance response using both sensing principles. Crack propagation in the CT specimen was simulated using a damage criteria and an element removal technique. Detailed description of this FE model can be found in reference [10].

The FE model was subjected to cyclic loading applied via the two circular holes, producing tensile strains in the crack tip region. Under this loading, a crack was generated which propagated along the highlighted elements in Fig. 2.5b. The crack resulted in a bi-directional and highly-localized strain field under the SEC sensor, as shown in Fig. 2.5c. The output database (ODB) file for the FE model contained all results for each element, including strain variations and initial element areas. These results were then entered into the equations (Eq. 2.3 and Eq. 2.8) for the two sensing principles to compute capacitance responses.

A comparison between the capacitance responses based on the original and revised sensing principles is shown in Fig. 2.6. 160 seconds of analysis was completed, which resulted in a 1.17 inch crack. Several typical crack lengths have been labeled in the figure along with the capacitance history. As shown in this figure, the capacitance responses calculated from the two sensing principles are nearly identical when the crack length is small. However, after the crack length reached a length approximately 0.68 in, the original sensing principle clearly underestimated the capacitance response. When the crack length reached 1.17 in at the end of the analysis, the original sensing principle underestimated the capacitance response by 40%. The study indicates that the revised sensing principle

provides more accurate capacitance calculation under large deformation since the higher order terms are kept in the equation.

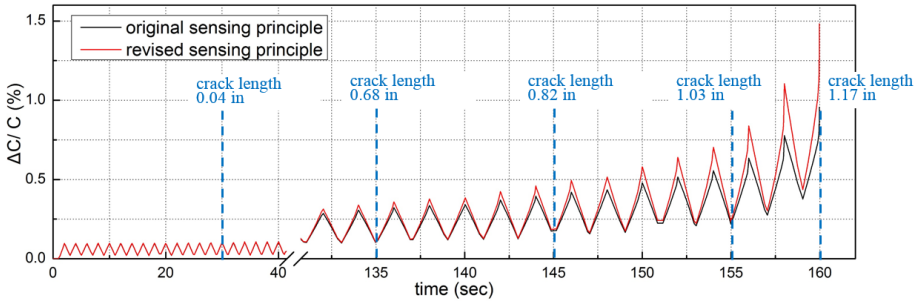

Figure 2.6 Capacitance responses from the original and revised sensing principles

3. EXPERIMENTAL TEST

In this section, a fatigue test of a steel CT specimen was carried out to demonstrate the characteristics of the SEC sensor for crack monitoring. The test design and setup are briefly described in Section 3.1. Then, some preliminary test results are shown in Section 3.2, including the full capacitance response of the SEC sensor in time domain, typical photographs for demonstrating crack propagation, and a developed relationship between capacitance change and crack length.

3.1. Test Design and Setup

An experimental study focused on crack monitoring using the SEC sensor was carried out by performing a fatigue test on a standard steel CT specimen. Similar tests were performed by Kharroub et al. [9]; however, only one crack size was measured for each test, making it difficult to quantify the relationship between crack size and capacitance measurement. The goal of this test was to closely observe the capacitance change while a crack propagated.

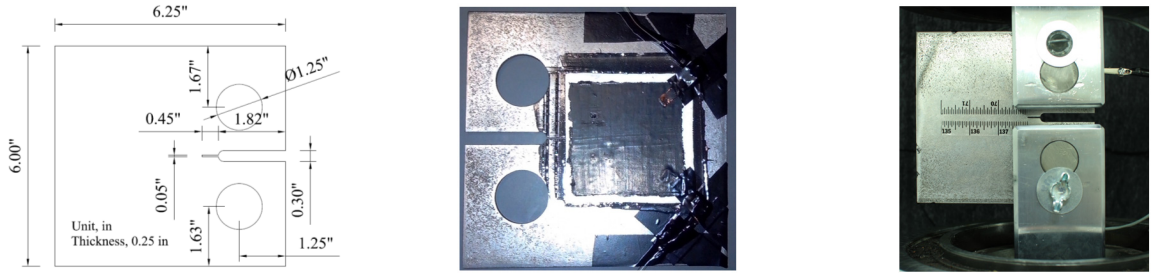

(a) (b) (c)

Figure 3.1 (a) Sizes of the specimen; (b) Sensor arrangement; and (c) adhesive tape measures

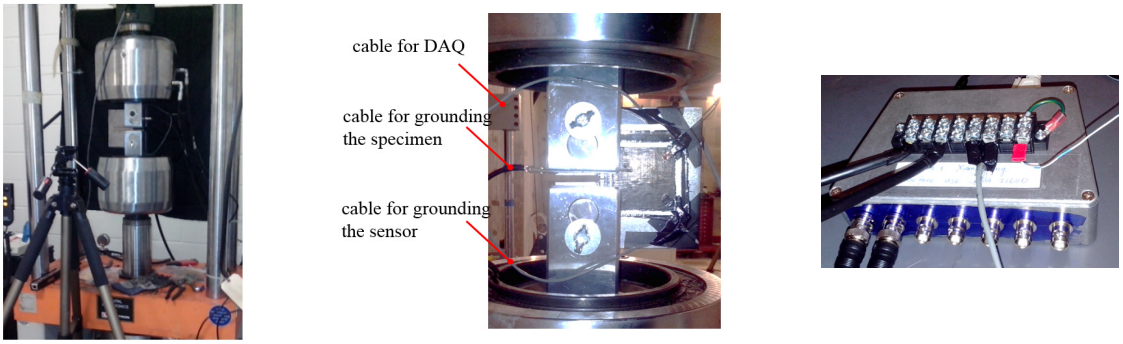

(a) (b) (c)

Figure 3.2 (a) Test setup; (b) cabling arrangement; and (c) DAQ box

The dimensions of the CT specimen are shown in Fig. 3.1a. The specimen was made of Gr. A36 steel with a thickness of ¼ in. To capture the crack growth, the specimen was first prepared by pickling with muriatic acid to remove mill scale, and was then polished with sandpapers. The SEC sensor was attached to one side of the specimen using a thin layer of epoxy (Fig. 3.1b). To measure crack size, pictures were taken by a Canon EOS

Rebel T2i camera and crack dimensions were obtained by counting pixels. Additionally, adhesive tape measures were attached alongside the expected crack path (Fig. 3.1c) as a secondary measurement technique for crack length. Each 1/16 in of crack propagation, the test was paused so that a high-definition photograph could be taken.

The CT specimen was mounted in an Instron uniaxial test machine (model 1334) via two clevises and rods (Fig. 3.2a). A tensile-tensile fatigue loading history was applied with a max and min amplitude of 6.5 kips and 0.65 kips, respectively. A 5 Hz loading frequency was used to initiate the crack, and then a loading frequency of 2 Hz was used while the crack propagated.

An off-the-shelf DAQ (ACAM PCap02) was used to measure capacitance response during the test. To reduce measurement noise, the DAQ board was sealed in an aluminum box (Fig. 3.2c) with signal and ground connectors exposed outside of the box. A BNC signal cable was connected to one pin of the SEC sensor while the other pin of the SEC and the specimen were both grounded (Fig. 3.2b).

3.2. Preliminary test results

The full time history of capacitance response is shown in Fig. 3.3a. The DAQ started to collect data when the crack length reached 3/16 in and continued recording data until failure. The total loading history lasted for about 50 minutes. Data collected during test pauses have been removed for clarity. The raw data was low-pass filtered with a 4 Hz cutoff frequency to smooth the curve. Some critical time points associated with different crack lengths have been marked in Fig. 3.3a. The specimen became unstable after the crack length reached 1-$^{9}/_{16}$ in, after which the specimen failed completely within a few cycles.

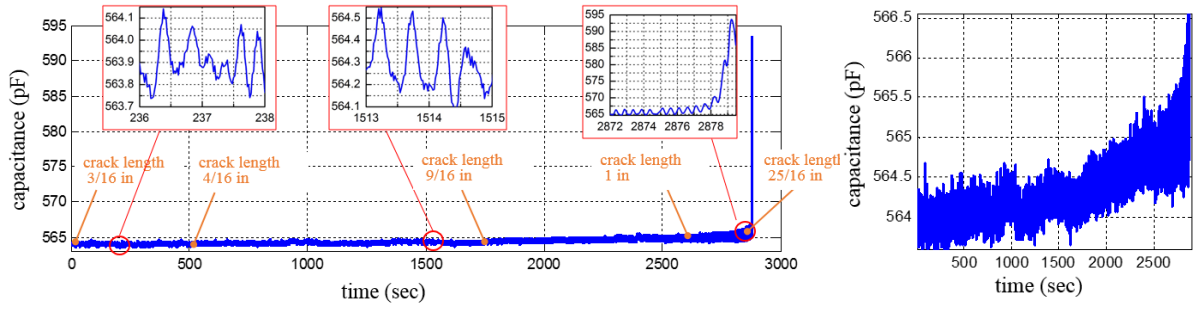

(a) (b)

Figure 3.3 Capacitance vs. time for (a) full time history; and (b) before crack length reached 1-$^{9}/_{16}$ in

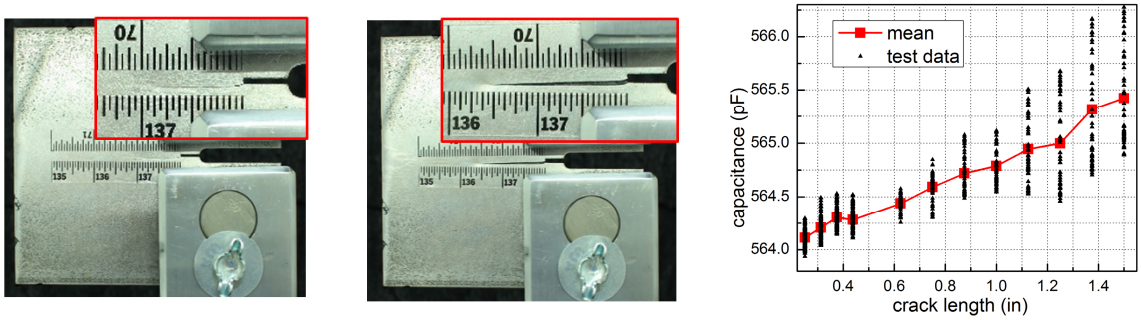

(a) (b) (c)

Figure 3.4 The CT specimen with crack length: (a) 1 in; (b) 1-$^{9}/_{16}$ in; and (c) capacitance vs. crack length

A steady growth of capacitance can be observed in Fig. 3.3a until the crack length reached 1-$^{9}/_{16}$ in. Fig. 3.3b shows the capacitance before cracking became unstable. The mean value of capacitance for each cycle increased from 563.9 pF at the beginning to 565.8 pF in the end. Furthermore, the amplitude of capacitance for each load cycle also increased from 0.8pF to 1.5 pF. Figs.3.4a and 3.4b show the pictures of specimen with a 1 in. and a 1-$^{9}/_{16}$ in. crack, respectively.

The relationship between crack length and the sensor's capacitance reading is presented in Fig. 3.4c. Due to measurement noise, the capacitance reading of the SEC sensor still experienced some variation even when the actuator was paused. Therefore, instead of using the data during the pauses, we choose the capacitance readings during the one second (2 loading cycles) just before each actuator pause (black dots in Fig. 3.4c), and then calculated the mean value of the readings to represent the mean capacitance associated with each crack length (red line in Fig. 3.4c). The curve in Fig. 3.4c shows a nearly linear relationship between capacitance and crack length. Moreover, the curve verifies that crack propagation can be monitored by capturing a steady increase of capacitance readings of the SEC sensor.

4. CONCLUSIONS

In this paper, characterization of the SEC sensor for fatigue crack monitoring was performed both numerically and experimentally. A revised sensing principle for the SEC was developed for accurate computation of capacitance based on FE analysis. An improved experimental program was also performed to quantify the relationship between crack size and capacitance response of the SEC sensor.

The revised sensing principle of the SEC sensor developed in this paper is particularly critical for crack detection, since cracking generates a highly localized and bi-directional strain field on a structural surface. The comparative study showed that both the original and revised sensing principles give similar capacitance response when the crack length is small (less than 0.68 in). However, the original sensing principle underestimated the capacitance response when the crack length became larger (1.17 in). These findings indicated the revised model has better performance on computing the capacitance response of the SEC sensor for large bi-directional deformations because of the retention of the higher order terms.

Aiming to depict the relationship between crack growth and sensor response, improvements were made in testing the CT specimen, including polishing the surface of the specimen, applying adhesive tape measures as reference for quantifying crack propagation in real time, reducing the load rate, and pausing the actuator multiple times for taking photographs. The relationship between crack length and capacitance changes demonstrated the SEC sensor's capability to monitor crack propagation by capturing a steadily increased capacitance response.

AKCNOWLEDGEMENT

This work was supported by the Iowa Department of Transportation (Iowa DOT) grant #RT454-494 and the Kansas Department of Transportation (KDOT). Their support is gratefully acknowledged. The authors would also like to acknowledge support provided through Pooled Fund Study TPF-5(328), which includes the following participating state DOTs: Kansas, Oklahoma, North Carolina, Minnesota, and Texas.

REFERENCES

1. Yao, Y., Tung, S. T. E., & Glisic, B. (2014). Crack detection and characterization techniques — an overview. *Structural Control and Health Monitoring.* **21(12)**, 1387-1413
2. Park, S., Yun, C. B., Roh, Y., & Lee, J. J. (2006). PZT-based active damage detection techniques for steel bridge components. *Smart Materials and Structures.* **15(4)**, 957
3. Roberts, T., & Talebzadeh, M. (2003). Acoustic emission monitoring of fatigue crack propagation. *Journal of Constructional Steel Research.* **59(6)**, 695-712
4. Kamaya, M., & Miyoshi, K. (2011). Monitoring of inside surface crack growth by strain measurement of the outside surface: a feasibility study. *Nuclear Engineering and Design.* **241(1)**, 1-11
5. Kamaya, M. (2013). Monitoring of inside surface crack growth by strain measurements of the outside surface: Application of multiple strain measurements technique to fatigue crack growth. *Nuclear Engineering and Design.* **256**, 202-213
6. Yao, Y., & Glisic, B. (2015). Detection of steel fatigue cracks with strain sensing sheets based on large area electronics. *Sensors*. **15(4)**, 8088-8108.
7. Laflamme, S., Kollosche, M., Connor, J. J., & Kofod, G. (2012). Robust flexible capacitive surface sensor for structural health monitoring applications. *Journal of Engineering Mechanics.* **139(7)**, 879-885
8. Laflamme, S., Saleem, H. S., Vasan, B. K., Geiger, R. L., Chen, D., Kessler, M. R., & Rajan, K. (2013). Soft elastomeric capacitor network for strain sensing over large surfaces. *Mechatronics, IEEE/ASME Transactions* on, **18(6),** 1647-1654
9. Kharroub, S., Laflamme, S., Song, C., Qiao, D., Phares, B., & Li, J. (2015). Smart sensing skin for detection and localization of fatigue cracks. *Smart Materials and Structures,* **24(6)**, 065004.
10. Kong, X., Li, J., Laflamme, S., Bennett, C., & Matamoros, A. (2015). Characterization of a soft elastomeric capacitive strain sensor for fatigue crack monitoring. *Proc. SPIE Smart Structures/NDE 2015, San Diego, CA*.
11. Laflamme, S., Wu, J., Song, C., Saleem, H., Uvertini, F. (2014). Study of the bidirectional sensing characteristic of a thin film strain gauge for monitoring of wind turbine blades, *6th World Conference on Structural Control and Monitoring*, Barcelona, Spain.